ON THE SOLUBILITY OF ALUMINIUM CARBIDE IN CRYOLITIC MELTS - INFLUENCE ON CELL PERFORMANCE

R. Ødegård, Å. Sterten and J. Thonstad

Laboratories of Industrial Electrochemistry and the Electrolysis Group of SINTEF*,

The Norwegian Institute of Technology, N-7034 Trondheim-NTH, Norway.

The solubility of aluminium carbide in cryolitic melts was determined as a function of NaF/AlF_3 molar ratio (CR), temperature, alumina concentration and CaF_2 concentration. At 1020°C a maximum concentration of 2.1 wt% aluminium carbide was found at CR=1.80. The following model for the aluminium carbide dissolution reaction based on activity data for NaF and AlF_3, was found to fit the experimental solubility data;

$$Al_4C_3(s) + 5AlF_3(diss) + 9NaF(\ell) = 3Al_3CF_8^{3-} + 9Na^+ \quad (1)$$

From the solubility data for aluminium carbide the following empirical equation was derived for CR>1.80:

$$\log(c_{Al_4C_3}) = -0.4149 - 0.3960 \cdot CR + 1.894 \cdot 10^3/T - 3.112 \cdot 10^{-2} \cdot c_{Al_2O_3} - 2.49 \cdot 10^{-2} \cdot c_{CaF_2} \quad (2)$$

where all concentrations are in wt% and T is the temperature (K).

Carbon could be electrodeposited from $NaF-AlF_3$ melts saturated with aluminium carbide by electrochemical oxidation of the dissolved carbide species whereby voluminous deposits of amorphous carbon were obtained.

INTRODUCTION

Although it is not always recognised by people involved in aluminium smelting, the solubility of aluminium carbide in cryolitic melts is a key issue in the electrowinning of aluminium. The aluminium carbide solubility necessitates a side ledge of frozen bath to protect the side walls of carbon in the cells, since this carbon lining, would deterioriate rapidly if freely exposed to aluminium and bath. To maintain a frozen side ledge of proper thickness precise control of the heat balance of the cells is required. Many of the well known cell control problems in aluminium electrowinning therefore originate from the need to avoid formation and dissolution of aluminium carbide.

Dewing [1] fitted experimental solubility data for aluminium carbide in $NaF-AlF_3$ melts to the empirical equation:

$$\log(\text{wt\% } Al_4C_3) = 1.298 - 0.587 \cdot (\text{molar ratio } NaF/AlF_3) \quad (3)$$

*: SINTEF = The Foundation for Scientific and Industrial Research at the Norwegian Institute of Technology.

The aluminium carbide solubility showed no temperature dependence in the temperature range 985-1080C°. Additions of up to 10 wt% of Al_2O_3, NaCl, CaF_2 or LiF had no influence on the measured solubilities, provided that LiF and CaF_2 were replaced by equivalent amounts of NaF when calculating the NaF/AlF_3 molar ratio (CR) used in eq. (1), [1].

For 2<CR<4.5 Dewing [1] obtained a good fit between the measured solubilities and the following dissolution reaction;

$$Al_4C_3 + 2AlF_3 = 3Al_2CF_2 \quad (4)$$

Electrodeposition of amorphous carbon has been reported both for cathodic polarization of the working electrode in molten carbonates [2,3,4] and by anodic polarization in melts containing dissolved CaC_2 [5,6]. In the latter case the overall anodic reaction was proposed to be [5];

$$C_2^{2-} = 2C(s) + 2e \quad (5)$$

The current for deposition of carbon from dissolved CaC_2 at 850°C was almost independent of stirring in the lower voltage range, while it increased at more positive potentials [5]. At higher temperatures (=1000°) the current increased with stirring also in the lower potential range [7]. These results indicate a shift from reaction control to diffusion control with increasing potential and temperature.

EXPERIMENTAL

A vertical tube furnace, of the type described by Motzfeld [8], with argon atmosphere was used for the aluminium carbide solubility measurements as well as the carbon deposition experiments. The temperature was measured with a standardized Pt·Pt10%Rh thermocouple and it was kept constant within ± 1°C.

The molten salt (≈140g, made up of high purity pre-dried components) and aluminium (=25g, +99.999% Al) were contained in graphite crucibles (44 mm i.d., CS, Union Carbide). In the solubility experiments crucibles with close-fitting lids of the same material were used. The crucibles were placed in the isothermal zone of the tube furnace. The melt was kept at temperature for a period of approximately 5 hours to ensure saturation with dissolved aluminium carbide formed by the reaction between aluminium and the graphite crucible.

In the solubility experiments the crucible lid was removed by means of a molybdenum wire attached to the lid. A melt sample (≈5g) was then taken, using a thick-walled steel ladle with a steel lid that was kept in the cold part of the furnace. The ladle was quickly lowered into the melt and then withdrawn to the cold zone. This was done without admitting air to the furnace tube. The quenched melt sample was kept in the cold part of the furnace for about five minutes and then quickly transferred to a glove-box with argon atmosphere (< 5ppm H_2O) where the sample was ground to -80 mesh. The sample was treated with a 10% HCl solution, and the total volume of gas evolved due to the reactions between the solution and aluminium carbide (CH_4) and aluminium (H_2) was determined volumetrically. The analysis apparatus was similar to that described by Rogers et al. [9]. When the gas evolution was completed, the evolved gas was analysed for methane and hydrogen by a gas chromatograph (Varion Aerograph, 90-P). In the calculation of the amount of dissolved aluminium carbide based on the volume of methane, corrections were made for temperature, atmospheric pressure, the partial pressure of water at the temperature of analysis, and the amount of dissolved metal in the melt sample.

In the carbon deposition experiments the graphite crucible was used as counter electrode (cathode) and a variety of electrode materials was applied as working electrode (anode). The aluminium pool (surface area ≈ 25 cm^2) with a tungsten rod (2 mm diam.) for electrical contact served as reference electrode.

In constant current experiments a DC power supply (Hewlett Packard 6274B) was used. The cell voltage and current were recorded on a two channel strip chart x-t recorder (W+W, 312). In potentiostatic measurements a high power potentiostat (Wenking HP72) with a potential scan generator (Wenking VSG72) was used. The current was recorded versus the working electrode potential on an x-y recorder (Watanabe WX4301). The IR-drop between the working and the reference electrodes was determined by means of a Solartron 1250 frequency response analyser.

After the deposition experiments samples for x-ray diffraction analysis (Philips PW 1730/10) were ground to -80 mesh and leached in a 30% $AlCl_3$ solution at 50°C for 24 hours to remove adhering salt. The samples were then washed in distilled water and dried at 150°C for 24 hrs. The same leaching and washing procedure was used for relatively large pieces of deposit (≈5 mm long) which were analysed on a scanning electron microprobe (ARL-SEM Q) and scanning electron microscope (JEOL, JSM-840).

RESULTS AND DISCUSSION

Solubility of aluminium carbide.

The concentration of dissolved aluminium carbide as a function of the NaF/AlF_3 molar ratio at 1020 ± 2°C is shown in Fig. 1. A representative selection of Dewing's [1] solubility data is also given in the figure. The broken line in the figure is a representation of Dewing's data in accordance with the present work showing a concentration peak of dissolved aluminium carbide with a maximum of 1.8 wt% Al_4C_3 at CR = 1.80. Because Dewing's measurements were not extended to low CR's the concentration peak shown in Fig. 1 was not detected in that work. For CR's between 1.8 and 4 the two curves show the same trend.

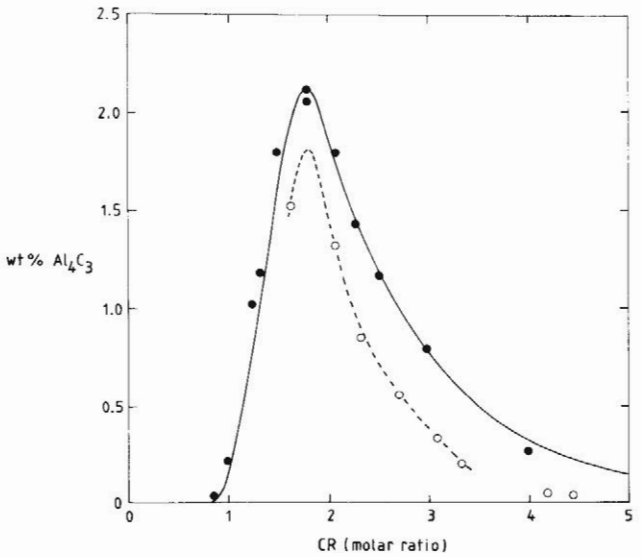

Fig. 1. Concentration of dissolved aluminium carbide in $NaF-AlF_3$ melts as a function of the NaF/AlF_3 molar ratio (CR) 1020 ± 2°C. ●: present work, o: Dewing [1]. The full line is based on a dissolution reaction according to eq. (8) (see text).

In the present work no variation was found in the amount of dissolved Al_4C_3 as a function of the saturation time (4-6 hrs). Also for the shortest holding time (4 hrs) intensely yellow coloured solid Al_4C_3 was found on almost the entire inner surface of the graphite crucibles after the experiments. Since Dewing used a 4 hrs holding time the discrepancy in the solubility data between the present work and those of Dewing [1] is therefore probably not due to differences in the degree of saturation. It can rather be due to different sampling procedures. In Dewing's work the whole crucible containing the melt (≈ 150 g) and aluminium (≈ 20 g) was quenched in tap water. Due to the fairly large mass to be quenched, this procedure probably gave a relatively low cooling rate with a possible loss of dissolved aluminium carbide due to coupled reactions like;

$$Al_4C_3(diss)+12NaF(l)=3C(s)+12Na(diss)+4AlF_3(diss) \quad (6)$$

and

$$Na(diss) = Na(g) \quad (7)$$

Another and perhaps more reasonable explanation is that Dewing [1] used rather concentrated H_2SO_4 to dissolve the melt samples. It is possible that some of the aluminium carbide in those samples was infact oxidized by the acid, leading to another hydrolysis product than methane.

The equilibrium vapour pressure of sodium increases with increasing CR [22], [13]. During a slow quenching the loss of dissolved aluminium carbide according to eqs. (6) and (7) would increase with increasing CR. In the present work the temperature of the ≈5g sample was recorded to be lower than 750°C within 3s after sampling. The loss of aluminium carbide during sampling was therefore believed to be small in the present work.

large number of dissolution models were tested [10] and the best fit to the experimental data was found for the reaction;

$$Al_4C_3 + 5AlF_3(diss) + 9NaF(\ell) = 3Al_3CF_8^{3-} + 9Na^+ \qquad (8)$$

This model is represented by the full line in Fig.1. Activity data for NaF and AlF_3 given by Sterten and Mæland [11] were used in the calculation which was based on the assumption of constant activity coefficient for $Al_3CF_8^{3-}$. Dewing's solubility model (Al_2CF_2), eq. (4), does not fit the data of the present work at low NaF/AlF_3 molar ratios. As mentioned a large number of other models were also tested, but none was found that gave nearly as good prediction of the concentration of dissolved aluminium carbide in $NaF-AlF_3$ melts as the model represented by eq. (8) does. This model is therefore adopted for the aluminium carbide dissolution reaction in $NaF-AlF_3$ melts. However, the presence of minor amounts of $Al_4CF_{12}^{4-}$ can not be excluded at low CR's (< 1.50). It should be emphasized that no spectroscopic study of the structure of dissolved aluminium carbide in cryolitic melts has been reported in the literature.

Fig. 2 shows the concentration of dissolved aluminium carbide as a function of temperature in $NaF-AlF_3$ melts with CR = 1.80. The concentration was found to decrease with increasing temperature from 2.96 wt% at 901°C to 1.77 wt% at 1062°C. Dewing [1] did not observe any significant temperature dependence of the concentration, and this could as mentioned above, be due to the difference in quenching procedure or to the difference in the analytical procedure.

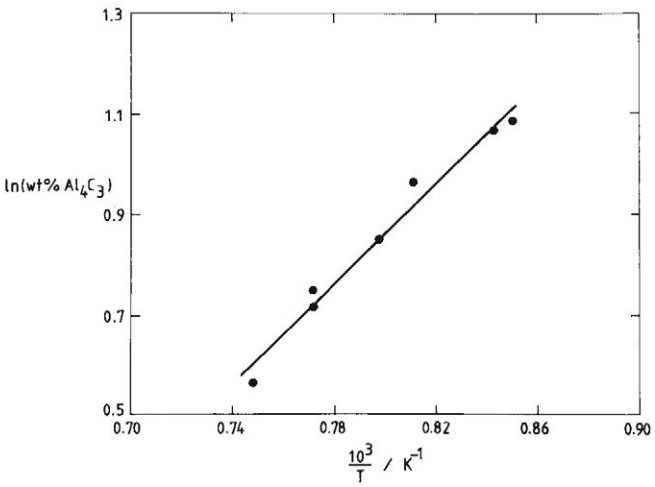

Fig. 2. The natural logarithm of the concentration of dissolved aluminium carbide as a function of the reciprocal temperature in $NaF-AlF_3$ melts at CR=1.80.

With the assumptions of ideal solution, no solid solution of aluminium carbide, and no difference in heat capacity between solid and liquid aluminium carbide the apparent heat of solution of aluminium carbide ($\Delta\bar{H}$) in $NaF-AlF_3$ melts at CR = 1.80 can be calculated from equation (9);

$$\ln\left(\frac{x}{x''}\right) = \frac{\Delta\bar{H}(T-T'')}{R \cdot T \cdot T''} \qquad (9)$$

where x is the mole fraction of Al_4C_3 at saturation, T is the temperature (K), and R is the gas constant. The calculation yields $\Delta\bar{H}$= - 41 kJ/mol. In the calculation the concentration in wt% was taken to be proportional to the mole fractions. This melt does not behave ideally [11], and the calculated heat of dissolution should only be regarded as an approximate value for the heat evolved during dissolution of aluminium carbide.

Fig. 3 shows the analysed concentration of dissolved aluminium carbide as a function of the alumina concentration in $NaF-AlF_3-Al_2O_3$ melts at CR = 1.80 and 1020 ± 2°C. In the calculation of the data in Fig. 3 the methane evolved during hydrolysis was formally treated as being caused only by dissolved Al_4C_3 (no oxy-carbides).

Contrary to the data of Dewing [1] which indicated no significant variation in the solubility of dissolved aluminium carbide with the alumina concentration, the present work shows a pronounced decrease in the aluminium carbide solubility with increasing concentration of alumina.

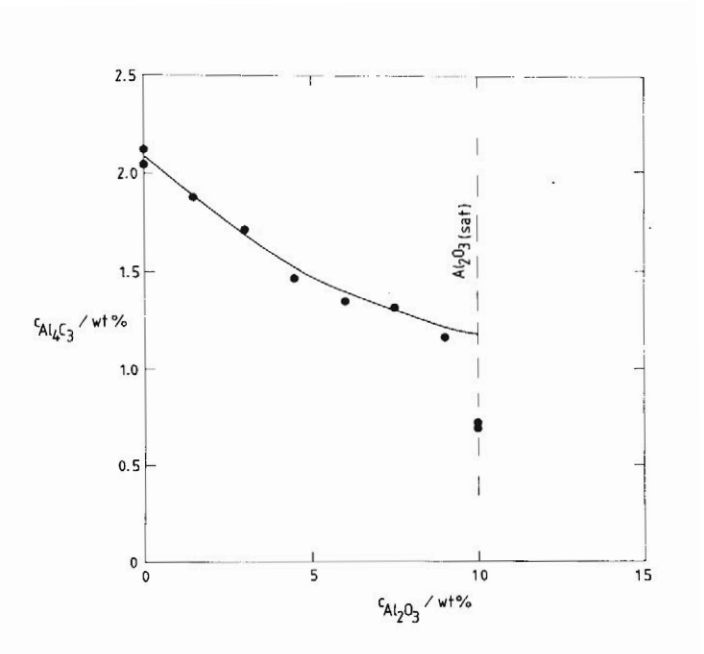

Fig. 3. Concentration of dissolved aluminium carbide as a function of the concentration of alumina in $NaF-AlF_3Al_2O_3$ melts at CR=1.80 and 1020 ± 2°C. (●): experimental data. The full line is based on calculated solubilities according to eq. (8).

Sterten and coworkers have given activity data for NaF and AlF_3 in alumina-saturated [13] and alumina-free [11] $NaF-AlF_3$ melts. The activities of NaF and AlF_3 were estimated as functions of the alumina concentration at CR = 1.80 and 1020°C. In the estimation the shape of the activity versus alumina concentration curves were assumed to be the same at CR = 1.80 as given by Sterten and Mæland [11] for CR = 3.00. The full line in Fig. 3 represents a model fitting based on dissolution of Al_4C_3 according to eq. (8) and the estimated activity data for NaF and AlF_3 as a function of the alumina concentration. In the model calculation the equilibrium constant used for eq. (8) was the same as that found to give the best fit in the pure $NaF-AlF_3$ system ($K_8 = 6.44 \cdot 10^{+6}$ at 1020°C).

Since the aluminium carbide dissolution according to eq. (8) has been found to agree well with the experimental data both in the pure $NaF-AlF_3$ system (Fig. 1) and in the $NaF-AlF_3-Al_2O_3$ system (Fig. 2), it should be reasonable to assume that the same model applies also to the $NaF-AlF_3-CaF_2$ system. However, the activities of NaF and AlF_3 as a function of CaF_2 addition are not known. In the following these activities are roughly estimated.

Fig. 4 gives the concentration of dissolved aluminium carbide as a function of the CaF_2 concentration in $NaF-AlF_3-CaF_2$ melts at CR = 1.80 and 1020°C ± 1°C. Dewing [1] found that addition of CaF_2 did not affect the aluminium carbide solubility provided that this addition formally was treated as an equivalent amount of NaF. The same model was tested in the present work and it is given as a broken line in Fig. 4. In the calculation of equivalent NaF/AlF_3 molar ratio with CaF_2 addition, one mole of CaF_2 was treated as being equivalent to two moles of NaF. The corresponding aluminium carbide solubility with addition of CaF_2 was then taken from Fig. 1. As can be seen from Fig. 4 the decrease in aluminium carbide solubility with addition of CaF_2 was considerably larger than that for an equivalent NaF addition in the present work.

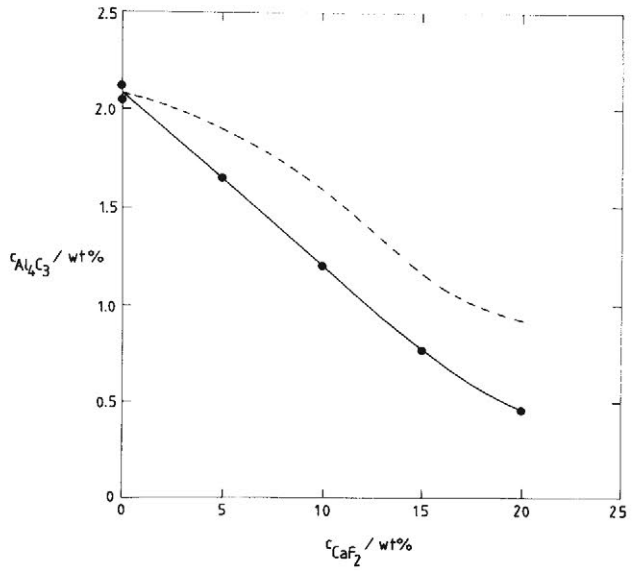

Fig. 4. Concentration of dissolved aluminium carbide as a function of the calcium fluoride concentration in $NaF-AlF_3-CaF_2$ melts at CR=1.80 and 1020°C ± 1°C. (●): experimental data. The dotted line represents CaF_2 treated as an equivalent NaF addition. The full line is calculated according to eq. (8) with estimated activity data for NaF and AlF_3. (For assumptions see text).

The occurrance of the $Al_2OC(s)$ compound reported by Grjotheim et al. [14] in experiments with cryolitic melts in presence of aluminium, carbon and alumina, is somewhat controversial since it is not stable in the pure $Al_4C_3-Al_2O_3$ system [15]. Grjotheim et al. claimed $Al_2OC(s)$ to be stable in cryolitic solutions at intermediate alumina concentrations since high alumina activity is expected to give $Al_4O_4C(s)$ and low alumina activity $Al_4C_3(s)$. The shape of the aluminium carbide solubility curve in Fig. 3 does not give any indication of a new species occurring at medium alumina concentrations. If $Al_2OC(s)$ were formed in the present experiments, the results strongly indicate that its presence does not affect the amount of dissolved carbide species.

Contrary to the treatment in the previous sections ,where literature data for the activities of NaF and AlF_3 were used in model fitting for the aluminium carbide solubility, the concentrations of dissolved aluminium carbide as a function of the CaF_2 concentration were used here to calculate the activities of NaF and AlF_3. In the calculations the melt was formally treated as being a mixture of $NaF_{(\ell)}$, $AlF_{3(diss)}$ and $CaF_{2(diss)}$.

The following equations were assumed for the variation of the activity coefficients of NaF and AlF_3 as a function of the CaF_2 concentration in $NaF-AlF_3$ melts:

$$\log\gamma_{NaF} = k_1 + k_2 \cdot x_{CaF_2} + k_3 \cdot x^2_{CaF_2} \quad (10)$$

$$\log\gamma_{AlF_3} = k_4 + k_5 \cdot x_{CaF_2} + k_6 \cdot x^2_{CaF_2} \quad (11)$$

where γ_{NaF} and γ_{AlF} are the activity coefficients of NaF_3 and AlF_3 respectively, and x_{CaF_2} is the mol fraction of CaF_2 in the melt. These assumptions are in accordance with model calculations in the cryolite system by, for example, Holm [29] and Dewing [30].

Activities for alumina-free melts given by Sterten and Mæland [11] were used to calculate k_1 and k_4. The aluminium carbide dissolution reaction according to eq. (8) was assumed for the $NaF-AlF_3-CaF_2$ system, and the equilibrium constant found to give the best fit in the pure $NaF-AlF_3$ system was used. The activities of NaF and AlF_3 were calculated by varying the constants in eqs. (10) and (11) to fit the experimental and calculated concentrations of dissolved aluminium carbide at all examined concentrations of CaF_2.

The best fit between the experimental solubility data and the calculated ones according to eq. (8) was found for:

$$\log\gamma_{NaF} = -0.7706 - 1.556 \cdot x_{CaF_2} - 4.0 \cdot x^2_{CaF_2} \quad (12)$$

$$\log\gamma_{AlF_3} = -1.714 + 2.800 \cdot x_{CaF_2} - 1.0 \cdot x^2_{CaF_2} \quad (13)$$

The solid line in Fig. 3 is based on eq. (8) and activities calculated by eqs. (12) and (13).

The calculated activities of NaF and AlF_3 as a function of CaF_2 addition are shown in Fig. 5. It should be emphasized that the calculation is based on the assumptions of aluminium carbide dissolution according to eq. (8) and activity coefficient variation in accordance with eqs. (12) and (13). The calculated activities must therefore only be taken as estimates, especially since the number of experimental solubility data with CaF_2 addition is only four. However, because the reduction in aluminium carbide solubility with CaF_2 addition is very pronounced, the trends in a_{NaF} and a_{AlF_3} as a function of the concentration of CaF_2 are believed to be correct. Consequently, CaF_2 seems to behave as a Lewis acid in this system.

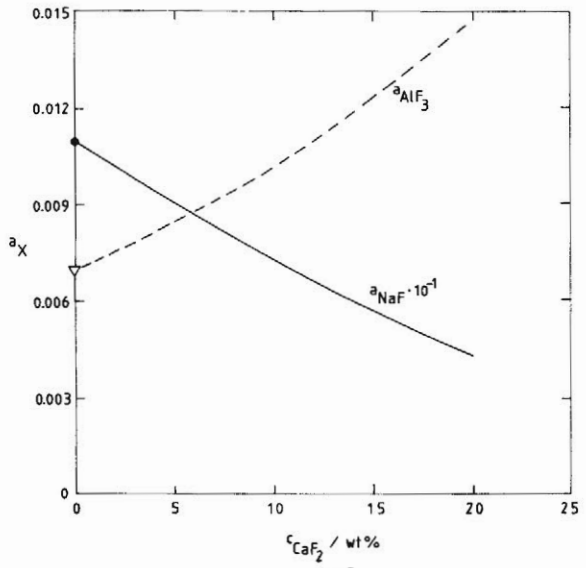

Fig. 5. Estimated activities of NaF and AlF_3 as a function of CaF_2 addition at CR = 1.80 and 1020°C.

1 2 3

Fig. 6. Carbon deposits on rods made of; 1: iron (3 mm), 2: vitreous carbon (3 mm) 3: tungsten (2 mm). CR=1.50, t=1000°C, total current 1-5 A.

Carbon deposition.

In electrolysis experiments with melts containing dissolved aluminium carbide, voluminous black deposits were obtained on the anode for all anode materials tested, i.e. graphite, vitreous carbon, iron, tungsten and platinum. The voltage was kept well below the decomposition voltage of alumina. In Fig. 6 is shown a photograph of deposits on tungsten, vitreous carbon and iron electrodes. Scanning electron microprobe analysis showed the deposit to be almost pure carbon (≈97 mole % C). The small fraction of non carbon materials was probably due to inclusions of salt, although the analyses were a little low in fluoride compared to the equivalent salt composition. Salt inclusions were also reported for deposition of carbon from dissolved CaC_2 in chloride melts [5].

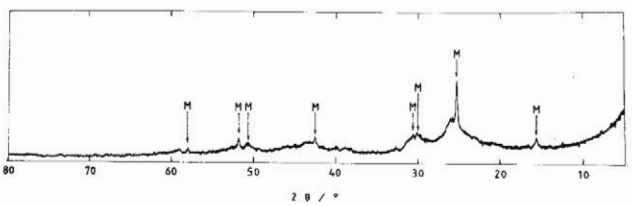

Fig. 7. X-ray diffractogram of electrodeposited carbon. Peaks marked "M" were identified as being due to salt compound ($NaAlF_4$, $Na_5Al_3F_{14}$). Deposition conditions: CR=1.50, t=1000°C, I=2A. Diffraction angle scan 5-80°.

Although deposition of carbon from the $NaF-AlF_3-Al_4C_3$ system has not been reported before to the authors' knowledge, some observation are mentioned in the literature that may be interpreted as indications of such a phenomenon. Sleppy and Cochran [16] observed "swelling" of the anodes during aluminium electrolysis in strongly acidic $NaF-AlF_3-Al_2O_3$ melts at 740°C (CR = 1.3). The relatively large increase in the diameter of the anodes could be interpreted as being due to carbon deposition. In the book; "Metallurgy of aluminium", by Beljajew et al. [17] is mentioned a tendency of "mushroom formation" ("spikes") on the anode(s) in aluminium cells with high contents of aluminium carbide.

Fig. 7 shows a typical x-ray diffractogram of the deposit. In spite of the fluoride extraction procedure described above, there are several peaks which originate from inclusions of melt remaining in the pores of the deposit. These peaks are marked by "M" in Fig. 7. The shape of the x-ray diffractogram indicates that the deposited carbon is amorphous.

From the weight loss when burning off electrodeposited carbon from a platinum electrode in air the number of electrons involved in the deposition reaction was calculated to be 4.31 and 4.44 in two experiments. The deviation from the expected number of four could be caused by a certain loss of carbon when taking the electrodes out of the furnace, and because a fraction of the current in the experiments will be used for oxidation of dissolved aluminium. Based on these experiments and on the model fitting for the aluminium carbide dissolution reaction (eq. (8)) the overall anodic reaction for aluminium carbide oxidation can be written;

$$Al_3CF_8^{3-} + F^- = C(s) + 3AlF_3(diss) + 4e \qquad (14)$$

Fig. 8 shows a typical potential decay curve recorded in carbon deposition experiments. A constant potential of 1.0 V was applied for two minutes and the current was then disconnected at time zero. The potential of the vitreous carbon electrode with carbon deposit on it was recorded

versus an aluminium electrode. The potential plateau which is clearly visible in Fig. 8, corresponds to an aluminium carbide formation cell with the reaction;

$$4Al(\ell) + 3C(s) = Al_4C_3(s) \quad (15)$$

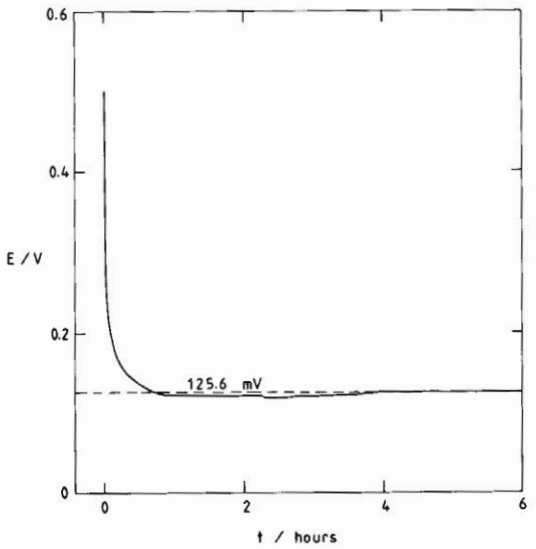

Fig. 8. Potential decay curve recorded after carbon deposition. The potential of a vitreous carbon electrode with carbon deposit on it was recorded versus an aluminium electrode.

The stable potential of the carbon electrode versus the aluminium electrode was +125.6 mV after correction for the thermoelectric potential measured in blank experiments at the temperature of the experiment (959°C). The Gibbs energy of formation of aluminium carbide can be calculated from the equation

$$\Delta G = -nFE \quad (16)$$

The Nernst equation can be written

$$E = E^{\circ} - \frac{RT}{nF} \ln \frac{a_{Al_4C_3}}{a_{Al}^4 \cdot a_C^3} \quad (17)$$

where $a_{Al} = a_C = 1$ (pure liquid aluminium and solid deposited carbon). Solid Al_4C_3 was found in the graphite crucibles after the deposition experiments. It is unlikely that the concentration gradients set up during electrolysis (≈1 A for 2 minutes) persisted for the duration the stable potential period (≃ 5 hours). Therefore, the shape of the potential curve in Fig. 8 strongly indicates that equilibrium was established between dissolved and solid aluminium carbide during this period. The activity of aluminium carbide is then taken to be unity. Hence E in eq. (17) is equal to the standard potential (E°) and $\Delta G_f^{\circ}, Al_4C_3$ can be calculated from eq. (16).

The value at 959°C is $\Delta G_f^{\circ}, Al_4C_3 = -145.425$ kJ/mol.

The corresponding thermodynamic data interpolated from the JANAF tables [18] is $\Delta G_f^{\circ}, Al_4C_3 = -147.936 \pm 7.90$ kJ/mol. The present value is also in reasonable good agreement with extrapolated data from Sandberg [19], $\Delta G_f^{\circ}, Al_4C_3 = -154.30 \pm 7.95$ kJ/mol.

Rey [20] suggested to use the aluminium carbide formation cell as a reference cell in $NaF-AlF_3$ melts. However, to the authors' knowledge, this is the first time the $Al/Al_4C_3/C$ formation cell has been shown to be stable for any length of time (see Fig. 8). The reason for the "undershoot" in potential in the beginning (≈7 mV after 2 1/2 hours) is probably pick-up of dissolved sodium [21] by the graphite electrode, resulting in non-saturation of dissolved aluminium at the graphite electrode. However, due to the resulting sodium gradient within the graphite electrode, the rate of sodium uptake will decrease with time, and after about 4 hours the aluminium activity apparently reached a steady level close to unity.

Similar to the observations of Morris and Harry [5] of anodic deposition of carbon from dissolved CaC_2, the morphology of the carbon deposit in the present work was found to change with the current density. Low current densities gave a dense deposit while a more "spongy" type of carbon was formed at high current densities. This is illustrated in Figs. 9 and 10 which show scanning electron micrographs (SEM) of electrodeposited carbon. The total electrolysis currents were equal to; 10.0 A and 1.0 A respectively. The other deposition conditions were identical for the two samples.

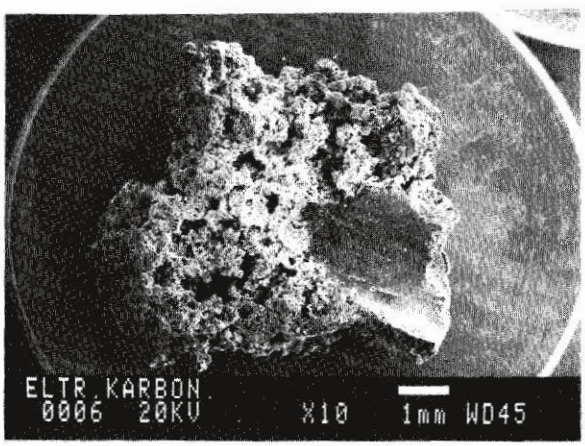

Fig. 9. SEM micrograph of electrodeposited carbon. Deposition conditions: I=10.0 A, t=1020°C, CR=1.50. The smooth area visible on the picture is the contact area to the vitreous carbon electrode (3 mm diam.).

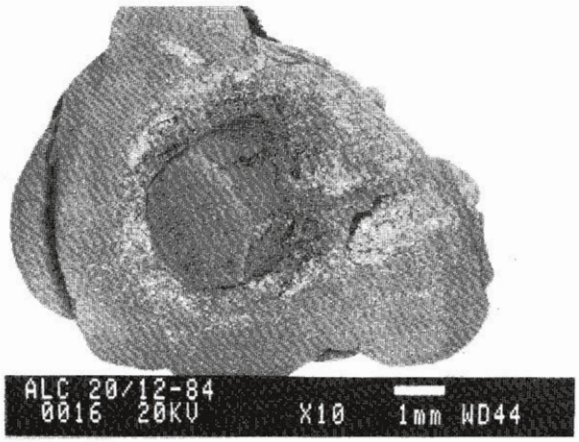

Fig. 10. SEM micrograph of electrodeposited carbon. Deposition conditions: I=1.0 A, t=1020°C, CR=1.50. The smooth area in the center of the sample is the contact area to the end of the vitreous carbon electrode (3 mm diam.).

SOME INDUSTRIAL IMPLICATIONS OF THE PRESENT WORK

The Aluminium Carbide Solubility.

From the solubility data for aluminium carbide, the following empirical equation was derived for CR > 1.80:

$$\log(c_{Al_4C_3}) = -0.4149 - 0.3960 \cdot CR + 1.894 \cdot 10^3/T$$

$$-0.3112 \cdot 10^{-2} \cdot c_{Al_2O_3} - 2.49 \cdot 10^{-2} \cdot c_{CaF_2} \qquad (18)$$

where $c_{Al_4C_3}$ is the concentration of dissolved aluminium carbide (wt%), $c_{Al_2O_3}$ is the concentration of alumina (wt%), c_{CaF_2} is the concentration of calcium fluoride (wt%), T is the temperature (K) and CR is the NaF/AlF_3 molar ratio.

Equation (18) was derived by multiple regression analysis, assuming that the activation energy for the aluminium dissolution reaction is independent of the composition, that the additives have the same relative effect at all CR's and temperatures, and that the effects of additions of CaF_2 and Al_2O_3 can be linearized.

With these assumptions eq. (18) is valid for 1.8 < CR < 4.0, the whole available range of temperatures and alumina concentrations, and for CaF_2 contents up to 10 wt%.

Equation (18) was derived by multiple linear regression analysis, and the correlation coefficient for all 20 measurements is 0.9939. The relative deviation between the equation and the measured solubilities was less than 10% for all measurements.

It should be stressed that eq. (18) cannot be applied for CR's below 1.80 since the concentration of dissolved aluminium carbide then starts to decrease (see Fig. 1), contrary to what eq. (18) might suggest. However, this should not be a problem when using eq. (18) to calculate the equilibrium concentration of dissolved aluminium carbide in industrial electrolytes since the equation covers a far wider range of CR's than used in commercial Hall-Héroult baths for aluminium production.

Dissolution and oxidation of aluminium carbide represent a reaction sequence that results in loss of current efficiency and the formation of carbon dust. Therefore, precautions should be taken to avoid aluminium carbide formation. Since unreacted carbon particles coming from the anode may react with dissolved aluminium forming aluminium carbide, it is important not to have anodes with large inherent variation in reactivity, which can give rise to disintegration of the anode. Furthermore, it is also of vital importance for the lifetime of Hall-Héroult cells to avoid deterioration of the side walls due to formation and dissolution of aluminium carbide [21,23]. In this respect it is important to maintain a proper side ledge of frozen cryolite in the cells. This will prevent direct contact between bath, liquid aluminium and the carbon side-lining and hence retard the formation of aluminium carbide.

Oxidation of dissolved aluminium carbide according to, for instance, eq. (16), will give relative large amounts of small, dispersed carbon particles in the bath (0.01-0.14 wt% C [24,25]).

$$Al_4C_{3(diss)} + 6CO_{2(g)} = 2Al_2O_{3(diss)} + 3C + 6CO_{(g)} \qquad (16)$$

Since aluminium carbide is formed from carbon and dissolved aluminium [26], the dispersed carbon may probably partly react with a stoichiometric amount of dissolved aluminium to form dissolved aluminium carbide. From the above mentioned analysis of dispersed carbon and the analysed equilibrium concentration of dissolved aluminium [27], one can calculate that this aluminium carbide formation reaction will result in a very low equilibrium concentration of dissolved aluminium in the bulk of the bath. The dissolution rate of aluminium is probably determined by the concentration gradient of aluminium across the diffusion layer at the aluminium cathode [28]. The aluminium carbide formation reaction in the bath will increase the dissolution rate of aluminium, by reducing the bulk concentration of aluminium, and hence decrease the current efficiency when compared to baths without dispersed carbon.

Equation (18) shows that low CR (high excess AlF_3 content), low alumina concentration and low temperature will give high equilibrium concentrations of dissolved aluminium carbide. In light of the above discussion, this phenomenon may represent an limitation to further improvement of the Hall-Héroult process by means of increasing the excess AlF_3 content in the bath beyond the present level of ≈12 wt%.

Electrodeposition of carbon.

Normally the carbon anodes in a Hall-Héroult cell are consumed at an average rate of ≈ 1.5 cm per day. Any carbon deposit resulting from oxidation of dissolved aluminium carbide at the anode surface may also be consumed in the same way. However, if the limiting current density for carbon deposition is higher than the local anodic

current density for CO_2 formation, which may be the case when the anode surface for some reason is partly blocked by, for instance, carbon dust or because of local depletion of alumina, then a net deposition reaction of carbon will take place. In this case carbon deposition will make the anode grow in those areas. This situation could be one reason for the formation of so-called "spikes" on the anode. The limiting current density for carbon deposition is probably proportional to the concentration of dissolved aluminium carbide. Based on the present aluminium carbide solubility data, one would expect an increased tendency to form "anode spikes" in Hall-Héroult cells when using a higher excess content of AlF_3, a lower temperature, or a lower alumina concentration. However, this statement should be regarded as a hypothesis, since, to the authors' knowledge, systematical observations of "anode spikes" in industrial cells have not been reported.

REFERENCES

1. E.W. Dewing, Trans.Metall. Soc. AIME, 245(1969), 181.
2. F. Haber, and S. Tolloczko, Z.Anorg.Chem., 41(1904), 412.
3. J. Dubois, Ann.Chim., t.10 (3-4)(1965), 145.
4. M.D. Ingram, B. Baron, and G.J. Janz, Electrochim.Acta, 11(1966), 1629.
5. D.R. Morris, and J.R. Harry, Proceeding of the International Conference on Industrial Carbon and Graphite (Society of Chemical Industry), London,1965,p.36.
6. S.H. White, and D.R. Morris, Proceedings of the Richardson Conference, Eds.; J.H.E. Jeffes and R.J. Tait, Inst. Min. Metall., London,1974,p.165.
7. D.R. Morris, "Ionic Carbides", in Molten Salt Technology, Ed: D.G. Lovering, Plenum Press, New York, 1982,p.153.
8. K. Motzfeldt, "Means of attending and controlling temperature", in Physiochemical Measurements at High Temperature, eds.: J.O'M. Bockrs, J.L. White and J.O Mackenzie, Butterworths, London,1959,p.51.
9. P.S. Rogers, D.J.M. Bevan and J.W. Tomlinson, Mikrochim.Acta, 12(1956), 1839.
10. R. Ødegård, On the Solubility and Electrochemical Behaviour of Aluminium and Aluminium Carbide in Cryolitic Melts, Dr.techn. thesis, The University of Trondheim, NTH, Norway,1986.
11. A. Sterten and I. Mæland, Acta Chem.Scand., A39(1985), 241.
12. G.N. Lewis and M. Randall, Thermodynamics, revised by K.S. Pitzer and L. Brewer, McGraw-Hill, New York, 1961.
13. Å. Sterten, K. Hamberg and I. Mæland, Acta Chem.Scand., A36(1982), 329.
14. K. Grjotheim, O. Herstad, R. Næumann and H.A. Øye, Light Metals 1978, 107th Annual Meeting of AIME, Denver, Colorado, 1978,Vol.1.,p.107.
15. K. Motzfeldt and B. Sandberg, Light Metals 1979, 108th Annual Meeting of AIME, New Orleans, 1979,p.411.
16. W.C. Sleppy and C.N. Cochran, Light Metals 1979, 108th Annual Meeting of AIME, New Orleans,1979,p.385.
17. A.I. Beljajew, M.B. Rapoport, and L.A. Firsanowa, Metallurgie des Aluminiums, (German translation), Vol.1., VEB Verlag Technik, Berlin,1956.
18. JANAF Thermochemical Tables, 2.ed., Dow Chemical Co., Midland, Michigan,1971.
19. B. Sandberg, Karbotemisk reduksjon av aluminiumoksyd, Dr.ing. thesis, The University of Trondheim, NTH, Norway,1981, (in Norwegian).
20. M. Rey, Electrochim.Acta, 14(1969), 991.
21. K. Grjotheim, C.Krohn, M. Malinovsky, K. Matiasovksky and J. Thonstad, Aluminium Electrolysis, 2.ed., Aluminium-Verlag, GmbH, Dusseldorf,1982.
22. H. Kvande, Thermodynamics of the System $NaF-AlF_3-Al_2O_3-Al$, Dr.techn. thesis, The University of Trondheim, NTH, Norway, 1979.
23. W.E. Haupin, The 3rd International Course on Process Metallurgy of Aluminium, Trondheim, 21-25 May,1984, p.9.40.
24. K. Grjotheim, C. Krohn and J. Thonstad, 5. Internationale Leichtmetalltagung, Leoben,1968,p.343.
25. T. Foosnæs, T. Naterstad, M. Bruheim and K. Grjotheim, Light Metals 1986, 115th Annual Meeting of AIME, New Orleans, 1986,p.729.
26. R. Ødegård and J. Thonstad, to be published.
27. R. Ødegård, Å. Sterten and J. Thonstad, "On the Solubility of Aluminium in Cryolitic Melts", to be presented at the 116th Annual Meeting of AIME, Denver, 1987.
28. K. Grjotheim, W.E. Haupin and B.J. Welch, Light Metals 1985, 114th Annual Meeting of AIME, New York, 1985,p.679.
29. J.L. Holm, Inorg.Chem., 12(1973), 2062.
30. E.W. Dewing, Light Metals 1985, 114th Annual Meeting of AIME, New York, 1985,p.737.